Analytical Potential Energy Surfaces for the Four-center Elimination Reaction of HCl from 1,1-Dichloroethylene: Translational Energy Release from Classical Trajectory Studies

Bong Woo Lee, Chang Hwan Rhee, and Hong Lae Kim*

Department of Chemistry, Kangwon National University, Chuncheon 200-701, Korea
Received March 29, 2000

Analytical potential energy surfaces have been constructed for the four-center elimination of HCl from 1,1-dichloroethylene. The potential functions are Morse-type functions which are modified by appropriate switching and attenuating functions with adjustable parameters. The parameters have been found by fitting the calculated vibrational frequencies, reaction endothermicity, equlibrium geometries of the reactant and products to those of experiments and *ab initio* calculations. The translational energy release obtained from classical trajectory calculations on this surface is in good agreement with the experiment.

Introduction

The molecular elimination processes in haloethylenes, $C_2H_{4-n}X_n$, are classified in three types: (1) the four-center elimination, also called α,β- or 1,2-elimination is a concerted, one-step reaction directly leading to the products, HCl and acetylene or haloacetylene; (2) the three-center elimination also referred to as α,α- or 1,1-elimination is a two-step reaction involving vinylidene or halovinylidene intermediates which rearrange to acetylene or haloacetylene; (3) the H or halide migration leading to haloethylidene intermediates, which are then dissociated into the products via the three-center elimination.

Morokuma *et al.*[1] studied potential energy surfaces for the unimolecular decomposition of dichloroethylene (DCE) and trichloroethylene in the ground electronic state by *ab initio* molecular orbital calculations. Experimentally, Umemoto *et al.*[2] measured translational energy (E_t) spectra of the Cl and HCl fragments from the $\pi^* \leftarrow \pi$ excitation at 193 nm from vinyl chloride, *trans*-DCE, *cis*-DCE, 1,1-DCE. The nascent rotational distributions of HCl ($\upsilon = 0$, 1, and 2) generated from the photodissociation of various isomers of DCE at 214 and 220 nm were also measured under molecular beam conditions.[3] The dissociation occurs in the ground electronic state via internal conversion. Gordon *et al.*[4] recently demonstrated that rotational energy distribution of HCl from the above dichloroethylenes is independent of the isomer of the parent molecule. The authors showed that only the four-center elimination takes place from 1,1-DCE. The measured rotational energy distributions of vibrationally excited HCl ($\upsilon = 1$ and 2) were Boltzmann-like, while those of HCl ($\upsilon = 0$) could not be represented by a single Boltzmann distribution which consisted of two components. The photodissociation of d_1-vinyl chloride was also investigated to elucidate the detailed dissociation mechanism of vinyl chloride.[5] It has been proposed that the product angular momentum distribution should be determined near the exit channel of the reaction coordinate and the very different rotational distribution observed in the case of HCl ($\upsilon > 0$) should be caused by formation of hydrogen-bonded π complexes between HCl and acetylene.

The detailed mechanism of the unimolecular dissociation of DCE can be understood from dynamics calculations. The first requirement for execution of computational studies is the construction of an acceptable potential energy surface to represent the 1,1-dichloroethylene system. For polyatomic molecules with many electrons such as DCE, this is a formidable task which can only be accomplished with limited accuracy. The size and number of *ab initio* calculations required to characterize the entire surface are too large. This is particularly true in a system where there exist several product channels and saddle point regions that are important for the dynamics of the reaction. In addition, the use of arbitrary functional forms selected to fit the *ab initio* results often leads to difficulties unless physically motivated forms are used.

The above considerations suggest that the most productive line of attack should be semi-empirical in nature. That is, a global representation of the potential energy surface should be searched which correctly reproduces as many of the known chemical features of the system as possible. These include the reaction endothermicity, the fundamental vibrational frequencies, and the equilibrium bond lengths and bond angles for all reactant and products. In addition, the surface should provide the correct reaction profile and barrier height. No matter what is done, however, the system is so complex that any global representation of the potential energy surface may necessarily be deficient in many respects. Nevertheless, if there are enough features of the surface that are in reasonable accord with experiments, then it should be possible to utilize the potential energy surface in various types of dynamics calculations.

In this paper, an analytical potential energy surface for the four-center elimination of HCl from 1,1-dichloroethylene is reported. In order to test usefulness of the surface, classical trajectory calculations have been performed on the constructed surface to determine the translational energy release from the reaction.

Calculations

***ab initio* Calculation**. The *ab initio* calculations were performed at the level of the second-order Mϕller-Plesset perturbation (MP2) using the 6-31G** basis in the GAMESS package.[10] The minimum energy geometries for the reactant and products were found with 1.0×10^{-7} hartree/bohr gradient convergence tolerance. The transition state geometry was determined under the same condition. To search for the transition state geometry, so-called the *standard method* implemented in the GAMESS package was used. Also, normal coordinate analysis was carried out at the same level to identify optimized stationary points, which was obtained by scaling the MP2 frequencies by 0.93. The structures and vibrational frequencies of the optimized geometries in the reaction of 1,1-DCE were summarized in Table 1, 2 and 3. The structure of the transition state obtained by the *ab initio* calculation is shown in Figure 1(b).

Verification of whether the transiton state structure does indeed connect the reactant and products requires calculation of the intrinsic reaction coordinate (IRC).[12-14] IRC connecting the reactant and products through the transition state was calculated using the Gonzalez-Schlegel second order (GS2) method in the GAMESS package. The gradient cutoff value of 1.0×10^{-7} hartree/bohr was used to determine whether IRC was approaching minima. The stride of 0.10 sqrt $\sqrt{amu} \cdot$ bohr was used to calculate the step length taken.

Analytical Potential Energy Surface. The atomic numbering adopted in the expression of the potential energy surface is shown in Figure 1. The total potential energy was expressed in terms of analytical functions of the interatomic distances and bond angles.[6-9] The energy minimum of the reactant is taken as the energy reference. The total potential energy is given by

Table 1. Harmonic frequencies (cm^{-1}) and geometries of the reactant

	MP2/6-31G**	Experimental[16]	Analytical Potential
ν_1 CH_2 s-stretch.	3058.15	3035	2987.71
ν_2 CC stretch.	1571.05	1627	1747.59
ν_3 CH_2 scis.	1341.86	1400	1336.44
ν_4 CCl_2 s-stretch.	586.22	603	509.38
ν_5 CCl_2 scis.	291.53	299	176.60
ν_6 Torsion	662.37	686	732.60
ν_7 CH_2 a-stretch.	3162.69	3130	3068.34
ν_8 CH_2 rock.	1056.30	1095	1084.89
ν_9 CCl_2 a-stretch.	773.76	800	825.05
ν_{10} CCl_2 rock.	352.46	372	260.13
ν_{11} CH_2 wag.	817.64	875	588.44
ν_{12} CCl_2 wag.	444.39	460	234.01
Å			
R_1 (C_1-C_2)	1.3345		1.3352
R_2 (C_1-H_1)	1.0781		1.0806
R_3 (C_1-H_2)	1.0781		1.0792
R_4 (C_2-Cl_1)	1.7267		1.7321
R_5 (C_2-Cl_2)	1.7267		1.7283
Degree			
θ_1 ($\angle C_2$-C_1-H_1)	120.25		124.84
θ_2 ($\angle C_2$-C_1-H_2)	120.25		119.34
θ_3 ($\angle C_1$-C_2-Cl_1)	122.56		123.35
θ_4 ($\angle C_1$-C_2-Cl_2)	122.56		121.97

Table 2. Harmonic frequencies (cm^{-1}) and geometries of the product

	MP2/6-31G**	Experimental[16]	Analytical Potential
CHCCl			
ν_1 CH stretch.	3284.43	3340	3361.58
ν_2 CC stretch.	2001.66	2110	2071.38
ν_3 CCl stretch.	708.35	756	636.99
ν_4 CH bend	496.08	604	1091.11
ν_5 CCCl bend	180.70	326	357.73
HCl			
ν	2880.46	2991	2793.94
Å			
CHCCl			
R_{CC}	1.2179		1.2180
R_{CH}	1.0616		1.0610
R_{CCl}	1.6456		1.6459
HCl			
R_{HCl}	1.2693		1.2740

Table 3. Harmonic frequencies (cm^{-1}) and geometries of the transition state

	MP2/6-31G**	Analytical Potential
ν_1 CH_2 s-stretch.	1462.16	2434.25
ν_2 CC stretch.	1856.63	1844.28
ν_3 CH_2 scis.	817.77	1454.77
ν_4 CCl_2 s-stretch.	677.14	649.72
ν_5 CCl_2 scis.	136.82	153.27
ν_6 Torsion	515.96	934.44
ν_7 CH_2 a-stretch.	3179.51	3439.84
ν_8 CH_2 rock.	1849.51 i	1533.38 i
ν_9 CCl_2 a-stretch.	439.15	494.41
ν_{10} CCl_2 rock.	310.53	274.49
ν_{11} CH_2 wag.	744.92	630.49
ν_{12} CCl_2 wag.	304.34	196.82
Å		
R_1 (C_1-C_2)	1.2600	1.2845
R_2 (C_1-H_1)	1.2409	1.2955
R_3 (C_1-H_2)	1.0735	1.1292
R_4 (C_2-Cl_1)	2.5757	2.6735
R_5 (C_2-Cl_2)	1.6206	1.7193
R_6 (H_1-Cl_1)	1.7385	1.9953
Degree		
θ_1 ($\angle C_2$-C_1-H_1)	90.75	151.85
θ_2 ($\angle C_2$-C_1-H_2)	139.75	139.62
θ_3 ($\angle C_1$-C_2-Cl_1)	86.51	59.37
θ_4 ($\angle C_1$-C_2-Cl_2)	167.83	167.18

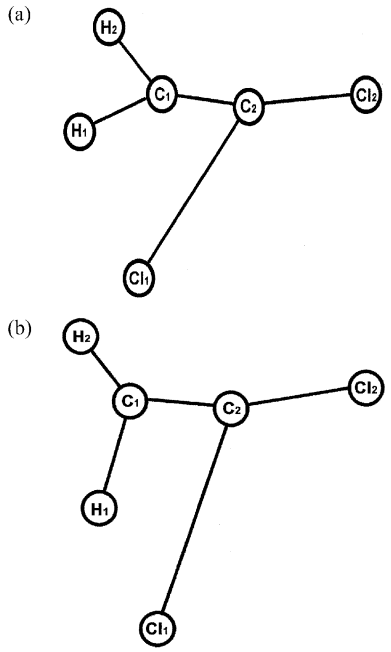

Figure 1. Optimized structures of 1,1-dichloroethylene at the transition state undergoing α,β HCl elimination reaction obtained by (a) the analytical potential energy surfaces and (b) the *ab initio* calculations.

$$V = V(R_{C_1C_2}) + V(R_{C_1H_1}) + V(R_{C_1H_2}) + V(R_{C_2Cl_1}) + V(R_{H_1Cl_1}) + \sum_{i=1}^{6} V(\theta_i) + \sum_{i=1}^{2} V(\alpha_i) + V_T(\phi) \quad (1)$$

The potential energy was chosen as the sum of bond stretching plus bending potential energies for each of the six angles along with wagging and torsional terms. Each of these potentials is multiplied by appropriate switching functions so as to provide correct asymptotic limits of the potential. In addition, each term is adjusted with parameters to allow the total potential to be fitted to the measured fundamental frequencies, equilibrium structures of the reactant and products, and the heat of reaction.

The carbon-carbon interaction, $V(R_{C_1C_2})$, is a Morse-type function whose parameters are varied with interatomic distances.

$$V(R_{C_1C_2}) = D_{CC}\left[e^{-2a_{CC}(R_{C_1C_2}-R^0_{CC})} - 2e^{-a_{CC}(R_{C_1C_2}-R^0_{CC})}\right] \quad (2)$$

where

$$D_{CC} = D^t_{CC} - (D^t_{CC} - D^d_{CC})SW(R_{C_1H_1}, R_{C_2Cl_1}, b_1, d_1) \quad (3)$$

$$\alpha_{CC} = \alpha^t_{CC} - (\alpha^t_{CC} - \alpha^d_{CC})SW(R_{C_1H_1}, R_{C_2Cl_1}, b_1, d_1) \quad (4)$$

$$R^0_{CC} = R^t_{CC} - (R^t_{CC} - R^d_{CC})SW(R_{C_1H_1}, R_{C_2Cl_1}, b_1, d_1) \quad (5)$$

with

$$SW(R_{C_1H_1}, R_{C_2Cl_1}, d_1, d_1) = \tanh^2\left(b_1 e^{-d_1(R_{C_1H_1} + R_{C_1Cl_1} - R^d_{CH} - R^d_{CCl})}\right) \quad (6)$$

In (3), D^t_{cc} and D^d_{cc} are the potential well depths for the carbon-carbon triple and double bonds, respectively. α^t_{cc} and α^d_{cc} are the curvature parameters and R^t_{cc} and R^d_{cc} are the equilibrium bond distances for the triple and double bonds, respectively, in (4) and (5). The switching function defined by (6) alters the Morse parameters of the carbon-carbon bond from those of the double bond to those appropriate for the triple bond as the reaction proceeds.

The interaction potential for the conserved carbon-hydrogen bond is given by

$$V(R_{C_1H_2}) = D_{CH}\left[e^{-2\alpha_{CH}(R_{C_1H_2}-R^0_{CH})} - 2e^{-2\alpha_{CH}(R_{C_1H_2}-R^0_{CH})}\right] \quad (7)$$

where

$$D_{CH} = D^t_{CH}(D^t_{CH} - D^d_{CH})SW(R_{C_1H_1}, R_{C_2Cl_1}, b_2, d_2) \quad (8)$$

$$\alpha_{CH} = \alpha^t_{CH}(\alpha^t_{CH} - \alpha^d_{CH})SW(R_{C_1H_1}, R_{C_2C_1}, b_2, d_2) \quad (9)$$

$$R^0_{CH} = R^t_{CH}(R^t_{CH} - R^d_{CH})SW(R_{C_1H_1}, R_{C_2Cl_1}, b_2, d_2) \quad (10)$$

with

$$SW(R_{C_1H_1}, R_{C_2C_1}, d_2, d_2) = \tanh^2\left(b_2 e^{-d_2(R_{C_2H_1} + R_{C_2Cl_1} - R^d_{CH} - R^d_{CCl})}\right) \quad (11)$$

As in (3)-(6), D^t_{CH} and D^d_{CH} are the well depths, α^t_{CH} and α^d_{CH} are the curvature parameters, α^t_{CH} and α^d_{CH} are the equilibrium bond distances between H and the triple and double bonded carbons, respectively.

The conserved carbon-chlorine interaction potential is given by

$$V(R_{C_2Cl_1}) = D_{CCl}\left[e^{-2\alpha_{CCl}(R_{C_2Cl_1}-R^0_{CCl})} - 2e^{-2\alpha_{CCl}(R_{C_2Cl_1}-R^0_{CCl})}\right] \quad (12)$$

where

$$D_{CCl} = D^t_{CCl} - (D^t_{CCl} - D^d_{CCl})SW(R_{C_1H_1}, R_{C_2Cl_1}, b_3, d_3) \quad (13)$$

$$\alpha_{CCl} = \alpha^t_{CCl} - (\alpha^t_{CCl} - \alpha^d_{CCl})SW(R_{C_1H_1}, R_{C_2Cl_1}, b_3, d_3) \quad (14)$$

$$R^0_{CCl} = R^t_{CCl} - (R^t_{CCl} - R^d_{CCl})SW(R_{C_1H_1}, R_{C_2Cl_1}, b_3, d_3) \quad (15)$$

with

$$SW(R_{C_1H_1}, R_{C_2Cl_1}, b_3, d_3) = \tanh^2\left(b_3 e^{-d_3(R_{C_1H_1} - R_{C_2Cl_1} - R^d_{CH} - R^d_{CCl})}\right) \quad (16)$$

The potential term between the carbon and departing hydrogen is

$$V(R_{C_1H_1}) = V_M(R_{C_1H_1})AT_1(R_{H_1Cl_1}, R_{H_1H_2}, R_{C_1C_2}, C_1, C_2, C_3) \quad (17)$$

where

$$V_M(R_{C_1H_1}) = D^d_{CH}\left(e^{-2\alpha^d_{CH}(R_{C_1H_1}-R^d_{CH})} - 2e^{-2\alpha^d_{CH}(R_{C_1H_1}-R^d_{CH})}\right) \quad (18)$$

$$AT_1(R_{H_1Cl_1}, R_{H_1H_2}, R_{C_1C_2}, C_1, C_2, C_3) = \left(1-e^{-C_1(R_{H_1Cl_1}-R^0_{HCl})^2}\right)\left(1-e^{-C_2(R_{H_1H_2}-R^0_{HCl})^2}\right) e^{-C_3(R_{C_1C_2}-R^0_{CC})^2} \quad (19)$$

This term is attenuated by $AT_1(R_{H_1Cl_1}, R_{H_1H_2}, R_{C_1C_2}, C_1, C_2, C_3)$ representing the interactions between the C_1 and C_2 whose distance becomes shorter, H_1 and Cl_1 approaching, and H_1 and H_2 pushing away each other as the reaction proceeds.

Also, $V(R_{C_2Cl_1})$ is the carbon-chlorine interaction term taken as

$$V(R_{C_2Cl_1}) = V_M(R_{C_2Cl_1})AT_2(R_{H_1Cl_1}, R_{Cl_1Cl_2}, R_{C_1C_2}, C_4, C_5, C_6) \quad (20)$$

where

$$V_M(R_{C_2Cl_1}) = D^d_{CCl}\left(e^{-2\alpha^d_{CCl}(R_{C_2Cl_1}-R^d_{CCl})^2} - 2e^{\alpha^d_{CCl}(R_{C_2Cl_1}-R^d_{CCl})}\right) \quad (21)$$

$$AT_2(R_{H_1Cl_1}, R_{Cl_1Cl_2}, R_{C_1C_2}, C_4, C_5, C_6) = \left(1-e^{-C_4(R_{H_1Cl_1}-R^0_{HCl})^2}\right)-\left(1-e^{-C_5(R_{Cl_1Cl_2}-R^0_{Cl_2})^2}\right) e^{-C_6(R_{C_1C_2}-R^0_{CC})^2} \quad (22)$$

The H-Cl bond forming interaction term is given by

$$V(R_{H_1Cl_1}) = \frac{1}{2}D_{HCl}\left(e^{-2\alpha_{HCl}(R_{H_1Cl_1}-R^0_{HCl})} - 2e^{-\alpha_{HCl}(R_{H_1Cl_2}-R^0_{HCl})}\right)\times AT_3(R_{C_1H_1}, R_{C_2Cl_1}, C_7) \quad (23)$$

where

$$AT_3(R_{C_1H_1}, R_{C_2Cl_1}, C_7) = 2-e^{-C_7(R_{C_1H_1}-R^d_{CH})^2} - e^{-C_7(R_{C_2Cl_1}-R^d_{CCl})^2} \quad (24)$$

The function is attenuated by the bond breaking carbon-hydrogen, carbon-chlorine interactions.

All the bending potentials have the quadratic form given by

$$V(\theta_i) = \frac{1}{2}k_{\theta_i}(\theta_i-\theta_{eq})^2 \quad (25)$$

where

$$k_{\theta_i} = k^0_{\theta_i}AT_{\theta_i}(R_j, R_k, \varepsilon_i) \quad (26)$$

$$\theta_{eq} = \theta^t_{eq} - (\theta^t_{eq}-\theta^d_{eq})SW_1(R_{C_1H_1}, R_{C_1Cl_1}, \Upsilon_i, \delta_i) \quad (27)$$

with

$$AT_{\theta_i}(R_j, R_k, \varepsilon_i) = e^{-\varepsilon_i((R_j-R^0_j)^2+(R_j-R^0_j)^2)} \quad (28)$$

$$SW(R_{C_1H_1}, R_{C_2Cl_1}, \Upsilon_i, \delta_i) = \tanh^2\left(\Upsilon_i e^{-\delta_i(R_{C_1H_1}+R_{C_2Cl_1}-R^d_{CH}-R_{CCld})}\right) \quad (29)$$

In (26)-(29), R_j and R_k are the two interatomic distances defining the angle θ_i while R^o_j and R^o_j are the corresponding equilibrium bond distances. θ^t_{eq} and θ^d_{eq} are the equilibrium angles. Eq. (26) attenuates the bending force constant as the reaction proceeds.

The alpha bending function is used for the wagging potentials taken as

$$V(\alpha_i) = \frac{1}{2}f_{\alpha_i}(\alpha_i-\pi)^2 \quad (30)$$

$$f_{\alpha_i} = f^0_{\alpha_i}AT_4(R_i, \lambda_i) \quad (31)$$

$$AT_4(R_i, \lambda_i) = e^{-\lambda_i(R_i-R^0_i)^2} \quad (32)$$

The torsional potential is given by

$$V_T^{CH_2CCl_2}(\phi) = \frac{1}{2}V_0(1-\cos 2\phi) \quad (33)$$

$$V_0 = V^\phi_0 AT_5(R_{C_1H_1}, \sigma) \quad (34)$$

$$AT_5(R_{C_1H_1}, \sigma) = e^{-\sigma(R_{C_1H_1}-R^0_{CH})^2} \quad (35)$$

where V^ϕ_0 is the torsional barrier height and ϕ is the dihedral angle with $\phi = 0$ for the planar conformation.

Eq. (1) contains 78 adjustable parameters, 23 of which are the equilibrium well-depth, curvature and bond distance parameters for the six possible diatomic pairs. For the well depth, curvature and equilibrium bond length of HCl, values from ref. 11 were used while for other bond length parameters, the *ab initio* results were used. In order to fit the reaction endothermicity and the vibrational frequencies of the reactant and products to the observed values, the equilibrium well depth and curvature parameters were adjusted. The parameters determined are listed in Table 4. The equilibrium bond angles of the *ab initio* results were used for the bending interactions and in order to fit the vibrational frequencies, the bending force constants were adjusted. The switching functions affect the rate of change of parameters from the reactant to the products. The attenuating functions affect the energy and structure of the transition state and the variation of the internal coordinates along the reaction path. To deter-

Table 4. Equilibrium Morse parameters for diatomic pairs

Diatomic pairs (α-β)	$D_{\alpha\beta}$ (kcal/mol)	$\alpha_{\alpha\beta}$ (Å^{-1})	$R^0_{\alpha\beta}$ (Å)
CC	225.09	2.20	1.218
C=C	184.03	1.95	1.334
≡C-H	123.14	1.88	1.061
=C-H	110.41	1.80	1.078
≡C-Cl	91.23	1.72	1.646
=C-Cl	80.24	1.66	1.727
H-Cl	97.16	1.86	1.274
H_2			0.742
Cl_2			1.988

mine these parameters, the bonding and the bending interactions were separated from the potential terms. The parameters of the bonding interaction were fitted by the internal coordinate variations on IRC from the *ab initio* calculation and the analytical potential surface. The parameters of the bending interactions were separated into the local modes of $-CH_2$ and $-CCl_2$ and were fitted by the internal coordinate variations of the analytical potential functions. For the other local modes collected by the wagging terms and the torsional terms, the parameters were adjusted to reproduce the vibrational frequencies. After fitting each local mode, concerning the bond forming and bond breaking, these parameters were adjusted until the results from IRC of the analytical potential energy surface was in good qualitative agreement with IRC of the *ab initio* calculation. The parameters thus obtained are listed in Table 5, 6, 7, respectively. The transition state structure was determined by the analytical potential energy surface using the *standard method* in the GAMESS package. IRC from the analytical potential energy surface was calculated using the constrained optimization method developed by Gonzalez and Schlegel. This is the same method used to obtain IRC from the *ab initio* calculation. Also, the same conditions for convergence were used in the calculation.

Table 5. Bending potential parameters

Angle α-β-Υ	$k^0_{\theta_i}$ ·(Å/rad^2)	θ^l_{eq} (deg.)	θ^d_{eq} (deg.)
H_1-C_1-H_2	0.295	0.00	119.50
C_2-C_1-H_1	0.523	180.00	120.25
C_2-C_1-H_2	0.523	180.00	120.25
Cl_1-C_2-Cl_2	0.232	180.00	114.86
C_1-C_2-Cl_1	0.350	0.00	122.57
C_1-C_2-Cl_2	0.350	180.00	122.57

Table 6. Wagging and torsional potential parameters

Wagging potential	Torsional potential
(mdyn · Å/rad^2)	
For H_2C=C	Torsion barrier
f^0 : 0.140	: 24.87 (kcal/mol)
For Cl_2C=C	
f^0 : 0.100	

Table 7. Switching, attenuating, wagging and torsional potential parameters

Parameter	Value	Parameter	Value	Parameter	Value
b_1	4.4	C_7	2.8	Υ_6	3.0
b_2	9.5	ε_1	1.8	δ_1	1.8
b_3	7.5	ε_2	12.0	δ_2	1.3
d_1	1.3	ε_3	1.0	δ_3	1.4
d_2	1.6	ε_4	1.2	δ_4	2.5
d_3	1.2	ε_5	1.3	δ_5	2.7
C_1	8.0	ε_6	1.0	δ_6	2.4
C_2	6.2	Υ_1	2.7	λ_1	2.0
C_3	0.1	Υ_2	2.0	λ_2	1.0
C_4	2.0	Υ_3	3.4	σ	1.0
C_5	9.0	Υ_4	3.2		
C_6	0.1	Υ_5	3.4		

Classical Trajectories. The classical Hamiltonian used in the trajectory calculation was written in terms of the absolute Cartesian coordinates.[6-9] In unimolecular reactions, it is necessary to sample high energy states of the molecules where the system is strongly coupled. The initial sampling requires to sample the initial Cartesian coordinates and momenta. However, a large number of degrees of freedom of the reactant molecule makes it difficult to study the unimolecular reactions. Hence, it is assumed that all the classical trajectories that lead to the elimination of products from the reactant should pass through the saddle point. Thus, an orthant-like sampling was carried out at the transition state structure to randomly select the initial momenta of the trajectories.[9] To conserve the total energy of the system, the initial momenta were scaled to the available kinetic energy $T(=E-V_{TS})$, where E is the sum of the initial rovibrational energy of the reactant and V_{TS} is the potential energy at the transition state. The initial rotational energy was sampled from thermal distribution at 300 K for a symmetric top following Hase.[9,15]

Integration of the classical equation of motion was done with the Gear's algorithm with an intermediate interval of 5.0×10^{-14} sec.[9] The 1352 trajectories were calculated at the initial vibrational energy of 153.56 kcal/mol (equivalent to the photon energy at 193 nm). Starting from the selected initial states, the trajectories were integrated until the complex was made (when the two fragments were 4 Å apart) or until the upper limit of 1 ps in time was exceeded. The length of the hydrogen bond in the complex is 3.70 Å, which is greater than the distance where HCl travels during the time of isomerization of vinylidene.[5] The results of the integration were checked at an interval of 1.0×10^{-15} sec. The energy conservation $|\Delta E|/E$ was $\sim 9 \times 10^{-5}$ at 153.56 kcal/mol after completion of the integration during 1 ps, which was the maximum integration time used in this study. From the trajectory results, the relative translational energy was calculated according to the method in the MERCURY program developed by Hase and co-workers.[15]

Results and Discussion

The potential energies from the *ab initio* calculations and

Table 8. Energies in kcal/mol from the *ab initio* calculations and from the analytical potential surface

	ab initio calcualtion	Analytical potential surface
barrier height	89.51	77.10
endothermicity	33.89	30.73
reverse barrier height	55.64	46.37

from the analytical potential surface are summarized in Table 8. The endothermicity is in good agreement with the experimental enthalpy at 298K, 27.9 ± 10.9 kcal/mol.[1] The large uncertainty in the experimental data comes from the large uncertainty in the enthalpy of formation of chloro- and dichloroacethylene.

The structures and vibrational frequencies of optimized geometries in the reaction of 1,1-DCE from the analytical potential surface were summarized in Table 1, 2 and 3. The structure of the transition state obtained by the analytical potential surface is shown in Figure 1(a). The α-β or four-center HCl elimination reaction takes place through planar transition state shown in Figure 1. In the initial stage of the reaction, the departing Cl atom travels toward the *cis*-H atom and reaches the transition state. The transition states from the *ab initio* calculations and from the analytical potential energy surface are very similar. The reacting C-Cl bond is already very stretched and is virtually broken. The reacting C-H bond is only slighty stretched and the HCl bond is still substantially longer than that in the free HCl molecule. The C-H bond breaking and the H-Cl bond formation take place after the transition state. This HCl elimination takes place maintaining the global C_s symmetry. Figure 2 shows IRC of the reaction calculated from the *ab initio* calculation and from the analytical potential energy surface. The overall shape of IRC of the analytical potential surface is in good agreement with the one from the *ab initio* calculations.

As can be seen in the tables, the vibrational frequencies and structural parameters of the species calculated by the *ab initio* and analytical potential surfaces are in good qualitative agreement while the energy, that is the barrier height and the structure of the transition state are somewhat different. Specifically, the departing H atom is closer to the departing Cl atom in the transition state calculated from the *ab initio* surface. However, as mentioned above, the overall mechanism of the reaction revealed by the two surfaces is exactly the same. The only references for the parameter fitting were the reaction endothermicity, vibrational frequencies and equilibrium structures of the reactant and products. Concerning the number of parameters to be determined, the calculated IRC from the analytical surface shows the similar shape to the one from the *ab initio* surface, although not quantitatively the same.

1592 trajectories were calculated at the energy of 153.56 kcal/mol and 57.6% of these were reactive. The average translational energy of the relative motion evaluated from the trajectories was 13.906 kcal/mol while 11.51 kcal/mol was measured from the experiment.[2] The translational

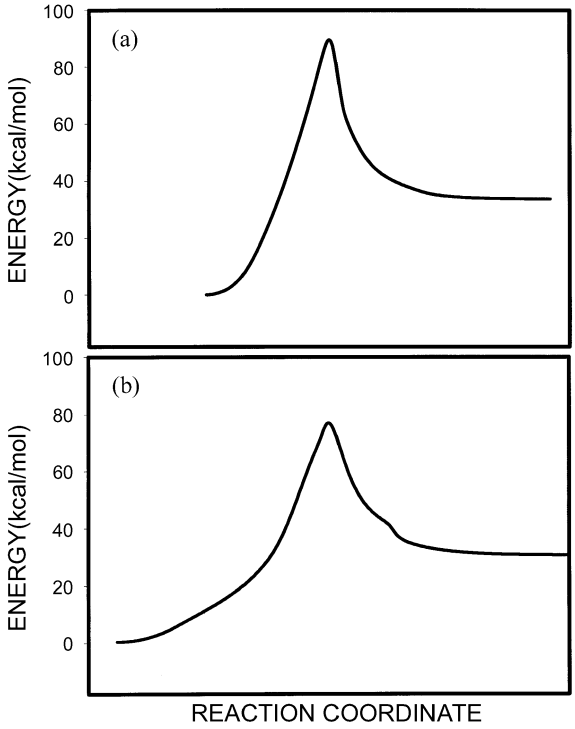

Figure 2. Potential energies along the minimum energy path for α,β HCl elimination reaction from 1,1-dichloroethylene obtained by (a) the *ab initio* calculations and (b) the analytical potential functions.

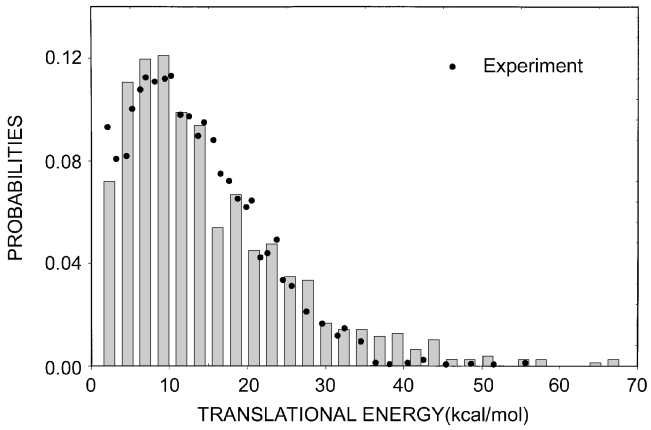

Figure 3. Translational energy distribution of HCl from α,β elimination reaction of 1,1-dichloroethylene calculated by classical trajectory calculations on the constructed analytical potential energy surfaces. The dots represent the experimentally measured distribution from ref. 2.

energy distribution of the relative motion is shown in Figure 3. Not only the average but also the overall shape of the relative translational energy distribution obtained by the classical trajectory calculation on the analytical potential surface is in excellent agreement with the experimental result. Since the product translational energy is determined by the transition state and the exit channel barrier, the analytical potential energy surface well explains the overall shape of the potential surfaces along the reaction coordinate in the exit channel.

Gordon *et al.*[5] have found that the elimination of HCl from d_1-vinyl chloride by a photon absorption followed by internal conversion occurs by α,α and α,β-elimination with the probabilities of 0.75 and 0.25, respectively. For the observed same rotational distributions of the products from the α,α and α,β mechanisms, they proposed that the rotational distribution is not determined until late in the reaction path. In this case, the final distribution is insensitive to the transition state. In addition, they have found that the difference between the rotational distributions in $\upsilon" = 0$ and $\upsilon" > 0$ is the same for both the α,α and α,β elimination. They proposed that this dichotomy may also be determined late in the reaction (exit channel effect). Such a process is suggestive of formation of a T-shaped HCl-C_2H_2 π complex in the product region, which was suggested by Morokuma *et al.* in their *ab initio* calculations[1]. A vibrationally excited HCl ($\upsilon" > 0$) moves more slowly and therefore, has a larger capture cross section by the sibling acetylene product than HCl ($\upsilon" = 0$), concerning the same total available energy. Thus, the HCl in $\upsilon" > 0$ has higher probability in forming the complex while the HCl in $\upsilon" = 0$ is mainly formed by the direct elimination from the chloroethylene. Once forming the complex, the subsequent decomposition should produce a Boltzmann-like rotational distribution, as contrasted by a non-Boltzmann distribution resulting from direct (concerted) elimination of HCl ($\upsilon" = 0$). So the rotational distribution of HCl in $\upsilon" = 0$ would have contributions from both the direct and complex mechanisms. Gordon *et al.* proposed that the rotational distribution of HCl is determined by the area of the potential energy surface in the exit channel.[5] However, our trajectory calculations on the constructed analytical potential energy surface was purely classical. Thus, the partitioning of the available energy into product internal degrees of freedom requires more elaborate semi-classical or quantal calculations. Moreover, a well by formation of the complex in the exit channel could not be considered in the constructed surface because such a well was not detected even by the *ab initio* the calculations. There should be somehow means of treating the small attractive interactions in the exit channel in performing the calculations. In this sense, the constructed analytical potential energy surface has to be modified in the product region, which needs more study in the future.

Acknowledgment. This work was financially supported by the non directed fund from Kangwon National University in Chuncheon, Korea.

References

1. Riehl, J.; Musaev, D. G.; Morokuma, K. *J. Chem. Phys.* **1994**, *101*, 5942.
2. Umemoto, M.; Seki, K.; Shinohara, H.; Nagashima, U.; Nishi, N.; Kinoshita, M.; Shimada, R. *J. Chem. Phys.* **1985**, *83*, 1657.
3. Sato, K.; Shihira, Y.; Tsunashima, S.; Umemoto, H.; Takayanagi, T.; Furukawa, K.; Ohno, S.-i. *J. Chem. Phys.* **1993**, *99*, 1703.
4. He, G.-x.; Yang, Y.-a.; Huang, Y.; Gordon, R. J. *J. Phys. Chem.* **1993**, *97*, 2186.
5. Huang, Y.; Yang, Y.-a.; He, G.-x.; Gordon, R. J. *J. Chem. Phys.* **1993**, *99*, 2752.
6. Benito, R. M.; Santamaria, J. *J. Phys. Chem.* **1988**, *92*, 5028.
7. Raff, L. M. *J. Phys. Chem.* **1987**, *91*, 3266.
8. Murrell, J. N.; Carter, S.; Farantos, S. C.; Huxley, P.; Varandas, A. J. C. *Molecular Potential Energy Functions*; Wiley: New York, 1984.
9. Lee, T. G.; Park, S. C.; Kim, M. S. *J. Chem. Phys.* **1996**, *104*, 4517.
10. Schmidt, M. W.; Baldridge, K. K.; Boatz, J. A.; Elbert, S. T.; Gordon, M. S.; Jensen, J. H.; Koseki, S.; Matsunaga, N.; Nguyen, K. A.; Su, S.; Windus, T. L.; Dupuis, M.; Montgomery, Jr., J. A. *J. Comp. Chem.* **1993**, *14*, 1347.
11. Persky, A.; Broida, M. *J. Chem. Phys.* **1984**, *81*, 4352.
12. Hase, W. L.; Feng, D.-f. *J. Chem. Phys.* **1974**, *61*, 4690.
13. Hase, W. L.; Feng, D.-f. *J. Chem. Phys.* **1976**, *64*, 651.
14. Sloane, C. S.; Hase, W. L. *J. Chem. Phys.* **1977**, *66*, 1523.
15. Hase, W. L.; Mrowka, G.; Brudzynski, R. J. *J. Chem. Phys.* **1978**, *69*, 3548.
16. Shimanouchi, T. *Tables of Molecular Vibrational Frequencies Consolidated Volume I*; Library of Congress Catalog Card Number: 66-60085.